Dear Editor and Reviewer,

We appreciate your constructive comments and thank you for the time spent on reviewing our revised manuscript. Your comments and suggestions have certainly improved the quality of the manuscript, which we greatly acknowledge. Please find below our detailed answers to the reviewer comments.

The manuscript have been revised by one reviewer. In their replies, the authors seems confident to be able to address the main issues raised during the reviewer process. After my own re-reading of the manuscript, I also have the following comments:

1.1- In the manuscript (abstract and introduction) the authors talk about parameters uncertainty and model uncertainty. Indeed in their application they only consider "parameter uncertainty" since only one model is considered. This point should be clarified in the manuscript. For example in the abstract the sentence "The model parameters and uncertainty " is misleading. I guess the authors mean "uncertainty in model parameters".

Reply 1.1:
Only one model is considered in this study and the uncertainty in model parameters is investigated. In the abstract and introduction, the wording has been changed to "uncertainty in the model parameters"

1.2- Introduction: page 2 last sentence "Generally ....analysis of parameter uncertainty and correlation is often left unaddressed". This statement is false. In the literature (and in particular in hydrology – hydrogeology) there is a large number of studies dealing with parameters uncertainty (starting at least from the '80).

Reply 1.2:
This is correct. Indeed, in hydrology and hydrogeology a large number of studies have addressed parameters uncertainty. However, in the case of EMI data analysis uncertainty in model parameters is often neglected, and this was the intent of the sentence here. We have addressed this by making a more specific statement.

1.3- Page 3, line 7 from the bottom "... to solve the full solution..."please rephrase

Reply 1.3:
In the revised manuscript the sentence has been rephrase as below:
"The alternative method used to calculate the forward EMI response is to solve the Maxwell's equation for the magnetic field measured over a horizontal layered medium, as proposed by Keller and Frischknecht (1966) and Anderson (1979)."

1.4- Page 4, eq (1). Symbol x not defined.
Reply 1.4:
Symbol "x" has now been defined as depth of the layer.

1.6- Page 4, line 6 from the bottom "....the prior distributions of a given model....". This sentence is not clear. Do you the authors mean the prior distributions of parameters a given model?

Reply 1.6:
The sentence was unclear and is now modified as below:
"Given a set of unknown parameters, the prior distributions of the model parameters are formulated and Bayes rule is then used to calculate posterior distribution conditioned on available observations (Arulampalam et al., 2002; Sivia, 2006)."

1.7- Page 5, symbol y two lines after eq (6) should not be in bold

Reply 1.7:
Bold option in the font settings has been deactivated for the symbol "y"

1.8- Eq (11). I am confused by this equation for the pdf of sigma. Sigma is defined as a positive (unbounded) variable. Therefore the integral of (11) between 0 and Infinity must be equal to 1. This is not true according to (11).

Reply 1.8:
Using the inverse gamma distribution, One gets

$$P(\sigma^2|\alpha,\beta) \propto (\sigma^2)^{-\alpha-1}\exp(-\frac{\beta}{\sigma^2})$$

Now taking β →0 and α →0 then the inverse gamma will approach the Jeffrey's prior. This distribution is called "uninformative" because it is a proper approximation to the Jeffreys prior

$$P(\sigma^2) \propto \frac{1}{\sigma^2}$$

which is uninformative for scale parameter, because this prior is the only one which remains invariant under a change of scale (note that the approximation is not invariant). This has a indefinite integral of $\log(\sigma^2)$ which shows that it is improper if the range of σ^2 includes either 0 or ∞. We don't observe infinite value for variance, and if the observed variance is zero, we have perfect data. So we can set a lower limit equal to L>0, and upper limit equal U<∞, and our distribution becomes proper. A better non-informative distribution can be chosen as the upper and lower limits L and U in the Jeffreys prior. Usually the limits can be set fairly easily with a bit of thought to what σ^2 actually means in the real world.

1.9- Page 6. The authors introduce the parameters to be estimated. These include (in the 3 layer system) 3 conductivities and only 2 layer thickness. Why the thickness of the third layer is not estimated?

Reply 1.9:
For the inversion algorithms of EMI data the thickness of the last layer is assumed to be infinite as the response of EMI signal is weak for deeper depths. This kind of approach is generally applied in EMI inversion studies such as those of Lavoué et al. (2010).

1.10- Page 8. Parameters sigma and sigma_b are not defined

Reply 1.10:
Sigma and sigma_b are now defined in the revised manuscript.

1.11- Page 8, line 8 from the bottom. Typo: replace siline by saline

Reply 1.11:
Typo mistake has been corrected.

1.12- Please consider to use the help of an expert in English usage and grammar to revise the manuscript

Reply 1.12:
The manuscript is now revised for English language by a native speaker.

1.13- If the authors decide to revise and resubmit the manuscript to HESS they should carefully address these issues together with the main criticisms pointed out by the reviewer.

The main criticisms pointed out by the reviewer were:
1.13a- "My only methodological issue with this paper. You use as non-conductive scenario a soil that is completely dry. (By the way, what are the salinity values measured at this site? E.g., the conductivity of the saturated paste extract?).
Reply 1.13a:
We thank the reviewer for highlighting this important issue. As reported in the last revision that for the same site, Jadoon et al. (2015) proposed a relationship to relate bulk electrical conductivity to the soil salinity (i.e., the conductivity of the saturated paste extract). Observed soil salinity range between 3-185 dS/m. In the last revision, the same relationship was used to estimate the soil salinity. Additional text and Figure 9 were incorporated to show the soil salinity distribution.

1.13b- In their protocols for use of apparent electrical conductivity measurements in agriculture, Corwin and Lesch state that the soil volumetric water content should be at least 50% of the value at field capacity (ideally between 70% and field capacity. Otherwise, the liquid pathways of electrical conductivity through the soils would be interrupted, unpredictably increasing the resistivity of the soil. This is very likely reason why your results on the non-conductive scenario are not encouraging.

Reply1.13b:
Indeed, in agriculture fields soil apparent electrical conductivity decreases if the soil volumetric water content decreases below 50% of the value at field capacity, whereby the process described by Corwin and Lesch greatly depends on soil textural distribution. Additionally, if non-saline water is used for irrigation the soil water content dominates the EC readings. In our study, on the other hand, saline groundwater was used to irrigate the Acacia tree and salt starts to accumulate in the top soil when volumetric soil water content decreases. Therefore, the accumulated salt has a dominating effect on soil apparent electrical conductivity and also the hydroscopic salts will provide liquid pathways even in this dry environment. Furthermore, in the field, non-conductive

soil were at locations between the Acacia trees where drip irrigation system was not used to irrigate the farm so there was no change in the soil water content for the non-conductive soil.

1.13c- My criticism is the following: with one scenario where ECa is known not to be reliable, is the other scenario (highly conductive medium) enough to provide context to your data analyses? I fear not. I think this paper would make much better of a point if other scenarios (e.g., increasing water contents?) were presented. See: Corwin, D.L., and S.M. Lesch. 2013. Protocols and guidelines for field-scale measurement of soil salinity distribution with ECa-directed soil sampling.
J. Environ. Eng. Geophysics 18(1):1-25. and: Corwin, D.L., and S.M. Lesch. 2005b. Characterizing soil spatial variability with apparent soil electrical conductivity: I. Survey protocols. Comput. Electron. Agric. 46(1-3):103-134."

Reply 1.13c:
In general, the protocols developed by Corwin and Lesch are mainly based on observations in combination with theoretical knowledge of current flow in porous media. Even if these protocols are of high value they are restricted to observational findings in specific environments. Therefore, we believe that a full physical description using synthetic scenarios in combination with observations will increase our understanding of EMI sensing for areas such as those being analysed here.
As such, the synthetic scenarios were analysed to test the performance of the electromagnetic forward model in conductive and non-conductive soil, with uncertainty in model parameters estimated using Bayesian inversion. In the case of synthetic scenario of non-saline soil, the increasing trend of soil moisture with depth has been analysed (Figure 1a). Results show that the electromagnetic forward model is not sensitive to the non-conductive soil. Previous studies have reported similar results for different EMI systems. For instance, Minsley (2011) used synthetic data considering the characteristics of shallow ground-based EMI system (Geophex GEM-2) and reported that the electromagnetic forward model is less sensitive to the non-conductive soil. While certainly very interesting, undertaking time-lapse EMI measurement with varying soil moisture dynamics is beyond the scope of this current contribution.

References:
Jadoon K. Z., Moghadas D., Jadoon A., Missimer T., Al-Mashharawi S., and McCabe M. F., 2015. Estimation of soil salinity in a drip irrigation system by using joint inversion of multi-coil electromagnetic induction measurements, Water Resources Research, volume 51, issue 5, page 3490-3504 DOI: 10.1002/2014WR016245

Minsley, B. J.: A trans-dimensional Bayesian Markov chain Monte Carlo algorithm for model assessment using frequency-domain electromagnetic data, Geophysical Journal International, 187, 252–272, 2011.

Lavoue, F., J. van der Kruk, J. Rings, F. Andre, D. Moghadas, J. A. Huisman, S. Lambot, L. Weihermuller, J. Vanderborght, and H. Vereecken (2010), Electromagnetic induction calibration using apparent electrical conductivity modelling based on electrical resistivity tomography, Near Surf. Geophys., 8(6), 553–561.

Manuscript prepared for Hydrol. Earth Syst. Sci.
with version 4.2 of the LaTeX class copernicus.cls.
Date: 17 May 2017

Inferring soil salinity in a drip irrigation system from multi-configuration EMI measurements using Adaptive Markov Chain Monte Carlo

Khan Zaib Jadoon[1], Muhammad Umer Altaf[2,3], Matthew Francis McCabe[2], Ibrahim Hoteit[3], Nisar Muhammad[1], and Lutz Weihermüller[4]

[1]Department of the Civil Engineering, COMSATS Institute of Information Technology, Abbottabad 22060, Pakistan
[2]Water Desalination and Reuse Center, King Abdullah University of Science and Technology (KAUST), Thuwal, 23955-6900, Saudi Arabia
[3]Earth Science and Engineering, King Abdullah University of Science and Technology (KAUST), Thuwal, 23955-6900, Saudi Arabia
[4]Agrosphere (IBG-3), Institute of Bio- and Geosciences, Forschungszentrum Juelich, GmbH, 52425 Juelich, Germany

Correspondence to: Khan Zaib Jadoon
(jadoonkz@ciit.net.pk)

Abstract. A substantial interpretation of electromagnetic induction (EMI) measurements requires quantifying optimal model parameters and uncertainty of a nonlinear inverse problem. For this purpose, an adaptive Bayesian Markov chain Monte Carlo (MCMC) algorithm is used to assess multi-orientation and multi-offset EMI measurements in an agriculture field with non-saline and saline soil. In MCMC the posterior distribution is computed using Bayes rule. The electromagnetic forward model based on the full solution of Maxwell's equations was used to simulate the apparent electrical conductivity measured with the configurations of EMI instrument, the CMD mini-Explorer. Uncertainty in the parameters for the three-layered earth model are investigated by using synthetic data. Our results show that in the scenario of non-saline soil, the parameters of layer thickness as compared to layers electrical conductivity are not very informative and are therefore difficult to resolve. Application of the proposed MCMC based inversion to field measurements in a drip irrigation system demonstrates that the parameters of the model can be well estimated for the saline soil as compared to the non-saline soil, and provides useful insight about parameter uncertainty for the assessment of the model outputs.

1 Introduction

Electromagnetic induction (EMI) with low frequency is a powerful tool to map the hydrological processes in the vadose zone due to the sensitivity to water content and soil salinity (Robinson et al., 2009). The use of EMI is largely motivated by the need of robust and compact system design, easy to use, rapid acquisition, and capability to provide a large set of georeferenced measurements, which can be associated with the spatial variability of subsurface at the field scale (Corwin, 2008). The EMI instrument is used to measure soil apparent electrical conductivity (EC_a), providing distribution of averaged electrical conductivity over a particular depth range. The depth of investigation of EC_a depends on the coil spacing, the coil orientation, and the frequency of the energizing field. Mester et al. (2011) reported that in the low induction number condition, the coil-orientation, offset, and frequency have major, moderate and minor effects on the penetration depth, respectively. Soil moisture, salinity and texture cannot be directly observed with EMI measurements. However, in non-saline soils, cation exchange capacity, soil moisture and texture are factors responsible for EC_a variations (Rhoades et al., 1976; Sudduth et al., 2003). Whereas in saline soil, the EC_a measurement is generally dominated by the soil salinity, and the reason is the accumulation of more salt concentration in the topsoil due to the loss of water through evaporation (Corwin and Lesch, 2005a,b; Ershadi et al., 2014). The success of EMI measurements to assess soil salinity depends on the establishment of site-specific petrophysical relationship to relate EC_a with the soil salinity estimated by electrical conductivity of the saturated paste extract (EC_e) (Cook and Walker, 1992).

Several inversion algorithms have been developed for EMI measurements to improve the resolution of subsurface features and the assessment of soil properties (Hendrickx et al., 2002; Santos et al., 2010; Triantafilis and Monteiro Santos, 2013). The majority of these inversion algorithms solve 1-D earth model for electromagnetic wave propagation. The model of McNeill (1980) has been extensively used for low induction number and Maxwell's equations has been utilized for high conductive soil ($EC_a >$ 100 mS/m) where the low induction number assumption is not valid. For example, Li et al. (2013) used Geonics EM38 to measure EC_a in a rice-paddy and inverted these using McNeill (1980) forward model to estimate the variation of soil salinity in a field condition. They reported that the yield reduced by 33% in an irregular shaped patch of strong saline topsoil.

EMI systems are sensitive to the field-specific calibration procedure, which limits the accuracy of EC_a measurements. In inversion modeling, however, precise measurements of EC_a is a prerequisite to characterize subsurface soil properties. For decades, the development and use of quantitative EMI inversions were mainly hampered by the lack of efficient calibration methods. von Hebel et al. (2014) used electrical resistivity tomography to calibrate EMI measurements before inversion to estimate three-dimensional images of subsurface electrical conductivity. Recently, Jadoon et al. (2015) calibrated EMI measurements via vertical electrical conductivity profile measured by capacitance sensors in different pits and later performed inversion for calibrated multi-configuration EMI measurements to estimate the effect of soil salinity distribution in an acacia tree farm.

EMI inversion algorithms are generally robust and provide useful estimates of subsurface properties in terms of optimal model parameters. Analysis of uncertainty in model parameters is however often left unaddressed. Parameters uncertainty can be associated with measurement errors (acquisition geometry, instrumental calibration and human error), modeling errors (assumptions in the electromagnetic forward model and petrophysical relationships), prior assumptions or constraints, parametrization, and estimation methods. Parameter uncertainty analysis can serve two main purposes: identify the model parameters of dominant importance, and provide confidence in the estimated model parameters (Scharnagl et al., 2011). For instance, Minsley (2011) used synthetic data considering the characteristics of the shallow ground-based EMI system, geophex GEM-2 (Huang and Won, 2003), to quantify parameters uncertainty of a three layer model via a Bayesian Markov Chain Monte Carlo (MCMC) approach. They show that combining multiple configuration EMI measurements significantly reduces total error, was best able to capture the shallow interface, and reduced regions of uncertainty at depth.

Conventional estimation of a single best-fit model with linear uncertainty does not usually trace ambiguity in the models, and may lead to a misguiding or imprecise interpretation. In this work, an adaptive Bayesian MCMC algorithm was used for inverting multi-orientation and multi-offset EMI measurements, in which the parameters posterior distribution represents the complete solution of the Bayesian inversion problem, including prediction of optimal parameters value and the associated uncertainty. Synthetic scenarios are first analyzed for a three-layered earth model to evaluate the uncertainty in model parameters for saline and non-saline soil using the characteristics of the CMD-Mini Explorer EMI system. Field measurements of the CMD-Mini explorer are then used to quantify parameters uncertainty in the three-layered earth model and soil salinity distributions in an agricultural field irrigated with drip irrigation system.

2 Materials and methods

2.1 Electromagnetic forward model

Forward EMI response for a given layered earth model is usually calculated by the McNeill (1980) model, which is generated using the cumulative electrical conductivity distribution over a certain depth range, and is valid under condition of low induction number. The alternative method used to calculate the forward EMI response is to solve the Maxwell's equation for the magnetic field measured over a horizontal layered medium (Keller and Frischknecht, 1966) and Anderson (1979). Preliminary analysis indicated that the electromagnetic forward model, which is based on high induction number assumption, returned more reliable apparent electrical conductivity values than the standard sensitivity curves of McNeill (1980). Furthermore, increased computational power made it possible to characterize the subsurface by utilizing forward models based on the Maxwell's equation (Santos et al., 2010). The effective depth of exploration is independent of EC_a in a low induction number condition, whereas in high induction number condition inverse relationship was found between the depth of exploration and EC_a (Callegary et al., 2007). For a combination of a vertical and horizontal dipole source-receiver with an offset ρ over a multilayered earth, the electromagnetic forward model can be written as:

$$EC_a^{HCP}(x,\rho) = \frac{-4\rho}{\omega\mu_0}\mathrm{Im}\left[\int_0^\infty R_0 J_0(\rho\lambda)\lambda^2 d\lambda\right], \tag{1}$$

$$EC_a^{VCP}(x,\rho) = \frac{-4}{\omega\mu_0}\mathrm{Im}\left[\int_0^\infty R_0 J_1(\rho\lambda)\lambda d\lambda\right]. \tag{2}$$

In these expressions, EC_a^{VCP} and EC_a^{HCP} represent apparent electrical conductivity - measured in vertical and horizontal coplanar mode, μ_0 represents permeability of the free space, λ indicates the radial wave number, J_0 and J_1 correspond to the zero-order and first-order Bessel functions, x is the depth of layer, ω is the angular frequency and Im the quadrature component. The reflection factor R_0 is obtained recursively, starting from the lowest layer N+1, with $R_{N+1} = 0$:

$$R_n(h_n,\sigma_n) = \frac{\frac{\Gamma_n - \Gamma_{n+1}}{\Gamma_n + \Gamma_{n+1}} + R_{n+1}\exp(-2\Gamma_{n+1}h_{n+1})}{1 + \frac{\Gamma_n - \Gamma_{n+1}}{\Gamma_n + \Gamma_{n+1}} R_{n+1}\exp(-2\Gamma_{n+1}h_{n+1})} \tag{3}$$

$$\Gamma_n = \sqrt{\lambda^2 + \omega\mu_0 j\sigma_n}, \tag{4}$$

$\sigma_0 = 0$, h_n is the height, and σ_n is the electrical conductivity for the n^{th} layer. This is based on the assumption that each layer is uniform with infinite horizontal extent. EMI measurements were carried out under high induction number conditions ($EC_a >$ 100 mS/m) utilizing the full solution of Maxwell's equation to model the forward EMI response.

2.2 Bayesian Inference

Bayesian inference is used to express the uncertainties in the system parameters based on a suitable likelihood function and a prior. Given a set of unknown parameters, the so called posterior distribution of the model parameters, which is the distribution of the parameters conditioned on available observations is calculated as the product of the prior distribution and the likelihood function (Arulampalam et al., 2002; Sivia, 2006). Bayesian inversion gained a lot of interests in recent years and has been applied in different applications, including climate, ocean and geophysical modeling (Malinverno, 2002; Zedler et al., 2012; Olson et al., 2012; Altaf et al., 2014; Sraj et al., 2014).

Suppose a set of observations ($\{y^i\}_{i=1}^n$) is available and assume a certain model to predict the data. Let α be the set of unknown parameters in the model, then according to Bayeś rule

$$p(\alpha|\{y^i\}_{i=1}^n) \propto p(\{y^i\}_{i=1}^n|\alpha)\, p(\alpha), \tag{5}$$

where $p(\alpha)$ is the prior distribution of α that represents the a priori knowledge about α, i.e. before considering the data. $p(\{y^i\}_{i=1}^n|\alpha)$ denotes the likelihood function: the probability of predicting the data given α. $p(\alpha|\{y^i\}_{i=1}^n)$ is the posterior probability: the probability of recovering α given the data ($\{y^i\}_{i=1}^n$).

Let's consider the forward model M, for the evaluation of the observations y as a function of the parameters such that:

$$y = M(\alpha). \tag{6}$$

Let ϵ be a random variable representing the discrepancy between our model $M(\alpha)$ and the observations, which we refer to as the observational noise:

$$\epsilon = y - M(\alpha). \tag{7}$$

Assuming the components of the observational noise to be independent and Gaussian of mean zero and variance σ^2, the likelihood function can then be decomposed as

$$p(\{y^i\}_{i=1}^n|\alpha) = \prod_{i=1}^n \frac{1}{\sqrt{2\pi\sigma^2}} \exp\left(-\frac{(y_i - M_i(\alpha))^2}{2\sigma^2}\right). \tag{8}$$

Here we consider σ^2 as an additional unknown (hyper) parameter and try to estimate its distribution as part of the inference process. The (joint) posterior distribution is then expressed as:

$$p(\alpha,\sigma^2|\{y^i\}_{i=1}^n) \propto \prod_{i=1}^n \frac{1}{\sqrt{2\pi\sigma^2}} \exp\left(-\frac{(y_i - M_i(\alpha))^2}{2\sigma^2}\right) p(\alpha)p(\sigma^2). \tag{9}$$

The choice of the prior is a key step in the inference process. Here, an informative uniform prior for all five (three conductivities and two thickness) parameters is considered, with α_k in the range $[\alpha_k^{max}\alpha_k^{min}]$; i.e:

$$p(\alpha_k) = \begin{cases} \frac{1}{\alpha_k^{max} - \alpha_k^{min}} & \text{for } \alpha_k^{min} < \alpha_k \le \alpha_k^{max}, \\ 0 & \text{otherwise.} \end{cases} \tag{10}$$

For the noise variance σ^2, we consider a Jeffreys prior (Sivia, 2006):

$$p(\alpha_k) = \begin{cases} \frac{1}{\sigma^2} & \text{for } \sigma^2 > 0, \\ 0 & \text{otherwise.} \end{cases} \tag{11}$$

The most commonly used computational strategy to numerically solve a multidimensional parameters Bayesian inference problem is the Markov Chain Monte Carlo (MCMC) method. We have applied an adaptive Metropolis MCMC algorithm to sample the posterior distribution, as discribed in details in Haario et al. (2001); Roberts and Rosenthal (2009)

2.3 Synthetic and Field Measurements

Two set of experimental setups were considered to test the MCMC approach and to evaluate the estimated model parameters and associated uncertainties using synthetic data for CMD Mini-Explorer configurations. Figure 1 (a) and (b) show a three-layer earth model setups of low and high conductivity for non-saline soil and saline soil salinity, respectively. In both setups, thicknesses for the three-layer earth model were conceptualized by a plow horizon (0.25 m thick), with an intermediate subsoil layer (0.50 m thick) and underlying consolidated layer up to 1.5 m depth. The plowing horizon generally has less soil moisture as compared to the deeper horizon because of evaporation and infiltration processes. The scenario of non-saline soil therefore used a plowing horizon with low electrical conductivity of 15 mS/m as compared to the intermediate and consolidated soil layers (Figure 1 (a)). In the saline soil scenario, salt accumulates on the surface of soil due to evaporation of water. As a result, the electrical conductivity of plowing horizon is considered higher 1800 mS/m as compared to the deeper layers (Figure 1 (b)). In the agricultural field, the increase in the soil salinity is generally due to the use of poor water quality or the excessive use of fertilizers. The forward response of both scenarios was calculated in HCP and VCP via Equations (1) and (2), respectively, for EMI configuration setups using the characteristics of CMD-Mini Explorer of three receiver coils respectively placed at 0.32, 0.71 and 1.18 m distances from the receiver.

In both scenarios, six configurations, three for each HCP and VCP with different spacings were taken as an output for forward models. Let $\alpha = (\sigma_1, \sigma_2, \sigma_3, h_1, h_2)^T$ be a vector of model parameters. σ_1, σ_2, and σ_3 are layer conductivities, and h_1 and h_2 thicknesses. Bayesian inference was used to estimate these 5 parameters that minimize the errors between observed and modeled HCP and VCP. An adaptive MCMC method was used to sample the posterior distributions and consequently update α distributions according to the observed data. All the results presented below are based on 10^4 MCMC samples. Parameter range for h_1 and h_2 was fixed between $0.05 - 0.6$ m in each scenario. In the non-saline scenario, parameter range for σ_1, σ_2 and σ_3 was considered between 5-100 mS/m and the saline soil scenario range was fixed between 5 - 3000 mS/m. A uniform prior distribution function was considered in both scenarios.

Field measurements were also carried out in a farm, where Acacia trees were irrigated with saline groundwater. The farm is located at a distance of 6 km from the Red Sea coast at Al-Qadeimah, Makkah province, Saudi Arabia. EMI measurements were collected at an interval of 2 m over a 40 m-long transect, along which three Acacia trees were irrigated using drip irrigation. At each location, EMI measurements using CMD-Mini explorer system gives six different values of apparent electrical conductivity (using two coil orientations and three offsets), each responds to different depth ranges. Ten pits were dug along the same transect and in each pit the bulk electrical conductivity σ_b profile was measured at 15 locations within a depth range of 0.05-1.5 m via 5TE capacitance sensors (Decagon Devices, Pullman, USA). EMI and 5TE measurements were performed 8 h after the drip irrigation system was stopped, so that the soil moisture is not concentrated below the drippers and to give enough time to reduce the soil moisture impact due to evaporation, root water uptake and infiltration (Jadoon et al., 2015).

3 Results and Discussion

3.1 Synthetic Data

Figure 2 (a) and (b) depicts the observed, estimated (modeled) and range of EC_a as they result from the chain of MCMC simulation for six configurations of the synthetic case with saline and non-saline soil. X-axis represents VCP and HCP with three coil spacing ($\rho 32$, $\rho 71$, $\rho 118$). In a non-saline scenario, the layer electrical conductivity increases with depth (Figure 1 (a)), and this is reflected in the observed and modeled EC_a in the VCP and HCP with increasing trend for larger spacing (Figure 2 (a)). The EC_a value for the VCP and HCP with maximum spacing of 1.8 m between transmitter and receiver corresponds to deeper horizon, in the case of saline soil scenario the layer conductivity decreases (Figure 1 (b)) and as a result EC_a values in VCP and HCP configuration exhibit a decreasing trend (Figure 2 (b)). The electromagnetic forward model is sensitive to high electrical conductive soil, so the modeled EC_a values for the saline soil scenario matches well with the observed as compared to the non-saline scenario. The mismatch between the observed and modeled EC_a values for non-saline soil is due to the weak sensitivity of the forward electromagnetic model to the low electrical conductivity.

Figure 3 (a) shows the true parameter values (red line) with the estimated parameters using MCMC (blue dash line) for the non-saline soil scenario. The MCMC samples were used to obtain the marginalized posterior distributions based on kernel density estimation (KDE) (Parzen, 1962). The 95 percent of the KDE for each parameter is shown by the shaded gray background (Figure 3 a). The resulting marginalized posterior pdfs of the three conductivities and two thicknesses are shown in Figure 3 (b $-$ f). The estimated parameters (Figure 3 b$-$f) show a single peak, corresponding to the best parameter values. The electrical conductivities of the three model layers (σ_1, σ_2 and σ_3) are reasonably well estimated as compared to the layer thicknesses. Different uniform prior distributions were also tested for the layer thicknesses, but the and MCMC solution converged close to the prior instead of the true layer thicknesses. The topography of the objective function was too flat in this case to allow consequent changes in the direction of layer thicknesses. This suggests that the electromagnetic model is not sensitive to the layer thicknesses for the low conductive soil layer.

Figure 4 illustrates the true and estimated depth profile of electrical conductivity for saline scenario, and the KDE of the marginalized posterior distributions for the three layer conductivities (σ_1, σ_2 and σ_3) and the two layer thicknesses (h_1 and h_2). The shaded gray background shows the 95 percent of the KDE for each parameter (Figure 4 a). The vertical electrical conductivity profile is well recovered by MCMC. The electrical conductivity of the top two layers are well estimated as compared to the consolidated layer with low electrical conductivity. Furthermore, for the six tested configurations of CMD Mini-Explorer, the HCP and VCP configuration with spacing 1.18 m are mostly sensitive to the consolidated layer while the remaining four configurations are more sensitive to the upper horizon. A large range of the parameter space was explored by MCMC (Figure 4 b − e), illustrating the sensitivity of the electromagnetic model to the considered parameters.

3.2 Experimental Data

Measurements were carried out in a farm, where acacia trees were irrigated with saline groundwater. The farm is located at a distance of 6 km from the Red Sea coast at Al-Qadeimah, Makkah province, Saudi Arabia. EMI measurements were collected at an intervals over a 40 m-long transect, along which three acacia trees were irrigated using drip irrigation. At each location, EMI measurements using the CMD-Mini explorer system provides six different values of apparent electrical conductivity (using two coil orientations and three offsets), each responds to different depth ranges. Ten pits were dug along the same transect and in each pit the vertical σ_b profile was measured at 15 locations within a depth range of 0.05-1.5 m via 5TE capacitance sensors (Decagon Devices, Pullman, USA). 5TE and EMI measurements were carried out on the same day 8 hr after the drip irrigation system was stopped, so that the soil moisture concentration below the drippers is avoided, and enough time is given for the reduction of soil moisture impact due to root water uptake, evaporation and infiltration (Jadoon et al., 2015).

Figure 5 shows the soil electrical conductivity measured in ten pits along a transect and the modeled soil electrical conductivity as estimated by the MCMC using the multi-configuration EM induction measurements. Pit locations along the transect are indicated by black triangle and cubic interpolation of 150 5TE sensor measurements were used to construct the two dimensional profile of measured soil electrical conductivity σ (Figure 5 (a)). The groundwater used to irrigate the acacia trees has an electrical conductivity of 4200 mS/m. The three patterns of high electrical conductivity is due to the infiltration front and soil salinity near the three acacia trees. In total, 21 multi-configuration EMI measurements were performed along a transect and calibrated with in situ measurements collected using capacitance sensors (Jadoon et al., 2015). The Three-layer earth model was considered for Bayesian inference of the five parameters (σ_1,σ_2,σ_3,h_1,h_2) and their uncertainty based on the 15,000 MCMC samples. For all MCMC simulations, the parameters search space was set relatively large, with the range of low and high values of electrical conductivity of soil; $0 < \sigma_1 < 3000$ mS/m, $0 < \sigma_2 < 3000$ mS/m, $0 < \sigma_3 < 3000$ mS/m, $0.05 < h_1 < 0.6$ m, and $0.05 < h_1 < 0.6$ m. In the depth section of soil electrical conductivity resulting from the EMI MCMC simulations, the effect of infiltration patterns and the soil salinity due to the drip irrigation near the three acacia trees is clear (Figure 5 (b)). The estimated soil electrical conductivity values by MCMC are in a good agreement with the sensor measurements performed in pits (Figure 5 (a)).

Figure 6 (a) and (b) show the measured, estimated (modeled) and range of EC_a as they result from the MCMC chain for the six multi-configuration of CMD-Mini Explorer for saline and non-saline soil. Three coil spacing for each VCP and HCP is represented on the x-axis. EMI measurement is shown for non-saline and saline soil at locations 4 and 9 of the pit (Figure 5 (a)), respectively. The soil was completely dry for non-saline soil as no irrigation was applied, whereas in the case of saline soil the moisture in the soil varied between 0.005 - 0.19 at the time of EMI and sensor measurements. In non-saline soil, the measured six EC_a values range between 5 - 60 mS/m and the modeled EC_a between 23 - 38 mS/m Figure (6 (a)). The range of EC_a estimated from the last 10,000 MCMC samples is in the range of 0 - 75 mS/m. As observed in the synthetic non-saline soil scenario, the electromagnetic forward model was not sensitive to the low electrical conductive soil. Similarly the fit between the measured and modeled EC_a is not in good agreement with the real measurements (Figure 6 (a)). Furthermore, the misfit may be due to the large search parameter space in the MCMC simulations. In the case of saline soil, the electrical conductivity of the top 50 cm soil is high due to the saline infiltration and soil salinity. This effect can be seen in the decreasing trend of the measured EC_a for the VCP and HCP measurements with larger coil spacing (Figure 6 (b)). The measured and modeled EC_a are in good agrement and this is due to the high sensitivity of the electromagnetic forward model to high electrical conductive soil.

Figure 7 plots the vertical profile of electrical conductivity for non-saline soil as measured by capacitance sensors (red line), the value of the MCMC estimated parameters (blue dash line), and the KDE of the marginalized posterior distributions for the three layer conductivities and the two layer thicknesses. The CMD-Mini Explorer measurements at the pit 4 for non-saline soil were used for the analysis. In Figure 7 (a) the measured vertical profile of soil electrical conductivity fall within the shaded area in the top 95% KDE distribution limits 0-0.7 m depth and below this depth the modeled soil electrical conductivity is overestimated. The mismatch between the measured and modeled EC_a for the maximum coil separation Hρ118 and Vρ118 is behind the overestimation of the soil electrical conductivity. The marginalized posterior pdfs of the three conductivities and two thicknesses are shown in Figure 7 (b $-$ f). The pdfs of the parameters (Figure 7 b$-$f) exhibit a single peak, corresponding to the best parameters. The peak of the σ_3 is flat between 30-38 mS/m and seems the topography of the objective function do not change within this range of conductivity in each iteration of the MCMC simulation.

Figure 8 plots the vertical profile of electrical conductivity for the saline soil measured by capacitance sensors (red line), the value of the MCMC estimated parameters (blue dash line), and the KDE of the marginalized posterior distributions for the three layer conductivities and the two layer thicknesses. CMD-Mini Explorer measurements at the pit 9 for the saline soil was used for the analysis. The shaded area in Figure 8 (a) indicates the 95% KDE distribution limits. The whole measured vertical profile of soil electrical conductivity fall within the shaded area, suggesting that the electrical conductivity is well estimated. The marginalized posterior pdfs of the three conductivities and two thicknesses, as shown in Figure 8 (b $-$ f), exhibit a single peak for all parameters except the layer thickness h_2 which is flat and suggest that the data were not informative to refine our prior knowledge about h_2. The posterior pdfs of the first two conductivities (σ_1 and σ_2) and layer thickness h_1 exhibit a clear Gaussian shape with an obvious Maximum A Posteriori (MAP). For the conductivity parameter σ_3, we notice a posterior with a well defined peak, but no standard pdf shape.

Figure 9 shows the spatial distribution of the soil salinity as estimated from EMI measurement using MCMC. Soil salinity EC_e is related to bulk electrical conductivity σ_b via a linear relationship ($EC_e = 13.74\sigma_b + 0.001$) established by Jadoon et al. (2015) for the same site. Infiltration front and high soil salinity range between 0.01 to 0.5 m at three locations where Acacia trees are irrigated with brackish water. The results show that the Bayesian inversion of multi-configuration EMI measurements successfully estimates the soil salinity caused by the brackish water infiltration. In the field, Acacia trees roots concentrated in the top 70 cm of soil and the low soil salinity below 30 cm show that Acacia are capable of extracting salt solutions and reduces subsoil salinity.

4 Conclusion

In this paper, an adaptive Bayesian MCMC algorithm has been implemented for the model assessment and uncertainty analysis of multi-orientation and multi-offset EMI measurements. The algorithm has been tested for CMD-Mini Explorer with both synthetic and field measurements conducted in an agriculture field over a non-saline and saline soil. Using Bayesian inference, marginalized posterior pdfs were computed for three subsurface electrical conductivities (σ_1, σ_2, and σ_3) and two layer thicknesses (h_1 and h_2) using MCMC. Such analysis helps to provide insight about parameters estimate and uncertainties.

The experimental results showed that the MCMC simulations can improve the reliability of the electromagnetic forward model to estimate the subsurface electrical conductivity profiles. Analysis shows that the electromagnetic forward model is less sensitive to the non-saline soil as compared to the saline soil. The proposed approach is flexible and can be implemented for various low-frequency ground-based EMI system and can provide subsurface electrical conductivity distribution and uncertainty of model parameters. Future research will focus to implement the Bayesian inference approach on time-lapse EMI measurements in different agricultural fields to monitor the soil dynamics, estimate the model parameters and their uncertainties.

Acknowledgements. This research was funded by the Water Desalination and Reuse Center, King Abdullah University of Science and Technology (KAUST), Saudi Arabia.

References

Altaf, M. U., Butler, T., Mayo, T., Luo, X., Dawson, C., Heemink, A. W., and Hoteit, I.: A Comparison of Ensemble Kalman Filters for Storm Surge Assimilation, Monthly Weather Review, 142, 2899–2914, 2014.

Anderson, W. L.: Numerical integration of related Hankel transforms of orders 0 and by adaptive digital filtering, Geophysics, 44, 1287–1305, 1979.

Arulampalam, M. S., Maskell, S., Gordon, N., and Clapp, T.: A tutorial on particle filters for online nonlinear/non-Gaussian Bayesian tracking, Ieee Transactions on Signal Processing, 50, 174–188, 2002.

Callegary, J. B., Ferre, T. P. A., and Groom, R. W.: Vertical spatial sensitivity and exploration depth of low-induction-number electromagnetic-induction instruments, Vadose Zone Journal, 6, 158–167, 2007.

Cook, P. G. and Walker, G. R.: Depth profiles of electrical-conductivity from linear-combinations of electromagnetic induction measurements, Soil Science Society of America Journal, 56, 1015–1022, 1992.

Corwin, D. L.: Past, present, and future trends of soil electrical conductivity measurement using geophysical methods, in: Handbook of Agricultural Geophysics, edited by Allred, B. J., D. J. J. E. M. R., pp. 17–44, CRC Press, Taylor and Francis Group, Boca Raton, Folrida, 2008.

Corwin, D. L. and Lesch, S. M.: Apparent soil electrical conductivity measurements in agriculture, Computers and Electronics in Agriculture, 46, 11–43, 2005a.

Corwin, D. L. and Lesch, S. M.: Characterizing soil spatial variability with apparent soil electrical conductivity: I. Survey protocols, Computers and Electronics in Agriculture, 46, 103–134, 2005b.

Ershadi, A., McCabe, M. F., Evans, J. P., Chaney, N. W., and Wood, E. F.: Multi-site evaluation of terrestrial evaporation models using FLUXNET data, Agricultural and Forest Meteorology, 187, 46–61, 2014.

Haario, H., Saksman, E., and Tamminen, J.: An adaptive Metropolis algorithm, Bernoulli, 7, 223–242, 2001.

Hendrickx, J. M. H., Borchers, B., Corwin, D. L., Lesch, S. M., Hilgendorf, A. C., and Schlue, J.: Inversion of soil conductivity profiles from electromagnetic induction measurements: Theory and experimental verification, Soil Science Society of America Journal, 66, 673–685, 2002.

Huang, H. P. and Won, I. J.: Real-time resistivity sounding using a hand-held broadband electromagnetic sensor, Geophysics, 68, 1224–1231, 2003.

Jadoon, K. Z., Moghadas, D., Jadoon, A., Missimer, T. M., Al-Mashharawi, S. K., and McCabe, M. F.: Estimation of soil salinity in a drip irrigation system by using joint inversion of multicoil electromagnetic induction measurements, Water Resources Research, 51, 3490–3504, 2015.

Keller, G. and Frischknecht, F.: Electrical methods in geophysical prospecting. International Series of Monographs in Electromagnetic Waves 10. Pergamon Press, Oxford, New York, 1966.

Li, H. Y., Shi, Z., Webster, R., and Triantafilis, J.: Mapping the three-dimensional variation of soil salinity in a rice-paddy soil, Geoderma, 195, 31–41, 2013.

Malinverno, A.: Parsimonious Bayesian Markov chain Monte Carlo inversion in a nonlinear geophysical problem, Geophysical Journal International, 151, 675–688, 2002.

McNeill, J. D.: Electromagnetic terrain conductivity measurement at low induction numbers, Tech note TN-6. Geonics Ltd., Mississauga, ON, Canada., 10, 1319–1330, 1980.

Mester, A., van der Kruk, J., Zimmermann, E., and Vereecken, H.: Quantitative Two-Layer Conductivity Inversion of Multi-Configuration Electromagnetic Induction Measurements, Vadose Zone Journal, 10, 1319–1330, 2011.

Minsley, B. J.: A trans-dimensional Bayesian Markov chain Monte Carlo algorithm for model assessment using frequency-domain electromagnetic data, Geophysical Journal International, 187, 252–272, 2011.

Olson, R., Sriver, R., Goes, M., Urban, N. M., Matthews, H. D., Haran, M., and Keller, K.: A climate sensitivity estimate using Bayesian fusion of instrumental observations and an Earth System model, Journal of Geophysical Research-Atmospheres, 117, 11, 2012.

Parzen, E.: On Estimation of a Probability Density Function and Mode, pp. 1065–1076, 1962.

Rhoades, J. D., Raats, P. A. C., and Prather, R. J.: Effects of Liquid-phase Electrical Conductivity, Water Content, and Surface Conductivity on Bulk Soil Electrical Conductivity, Soil Sci. Soc. Am. J., 40, 651–655, 1976.

Roberts, G. O. and Rosenthal, J. S.: Examples of Adaptive MCMC, Journal of Computational and Graphical Statistics, 18, 349–367, 2009.

Robinson, D. A., Lebron, I., Kocar, B., Phan, K., Sampson, M., Crook, N., and Fendorf, S.: Time-lapse geophysical imaging of soil moisture dynamics in tropical deltaic soils: An aid to interpreting hydrological and geochemical processes, Water Resources Research, 45, 12, 2009.

Santos, F. A. M., Triantafilis, J., Taylor, R. S., Holladay, S., and Bruzgulis, K. E.: Inversion of Conductivity Profiles from EM Using Full Solution and a 1-D Laterally Constrained Algorithm, Journal of Environmental and Engineering Geophysics, 15, 163–174, 2010.

Scharnagl, B., Vrugt, J. A., Vereecken, H., and Herbst, M.: Inverse modelling of in situ soil water dynamics: investigating the effect of different prior distributions of the soil hydraulic parameters, Hydrol. Earth Syst. Sci., 15, 3043–3059, 2011.

Sivia, D. S.: Data Analysis: A Bayesian Tutorial, Oxford Science Publications, Oxford, UK, 2006.

Sraj, I., Mandli, K. T., Knio, O. M., Dawson, C. N., and Hoteit, I.: Uncertainty quantification and inference of Manning's friction coefficients using DART buoy data during the Tohoku tsunami, Ocean Modelling, 83, 82–97, 2014.

Sudduth, K. A., Kitchen, N. R., Bollero, G. A., Bullock, D. G., and Wiebold, W. J.: Comparison of electromagnetic induction and direct sensing of soil electrical conductivity, Agronomy Journal, 95, 472–482, 2003.

Triantafilis, J. and Monteiro Santos, F. A.: Electromagnetic conductivity imaging (EMCI) of soil using a DUALEM-421 and inversion modelling software (EM4Soil), Geoderma, 211, 28–38, 2013.

von Hebel, C., Rudolph, S., Mester, A., Huisman, J. A., Kumbhar, P., Vereecken, H., and van der Kruk, J.: Three-dimensional imaging of subsurface structural patterns using quantitative large-scale multiconfiguration electromagnetic induction data, Water Resources Research, 50, 2732–2748, 2014.

Zedler, S. E., Kanschat, G., Korty, R., and Hoteit, I.: A new approach for the determination of the drag coefficient from the upper ocean response to a tropical cyclone: a feasibility study, Journal of Oceanography, 68, 227–241, 2012.

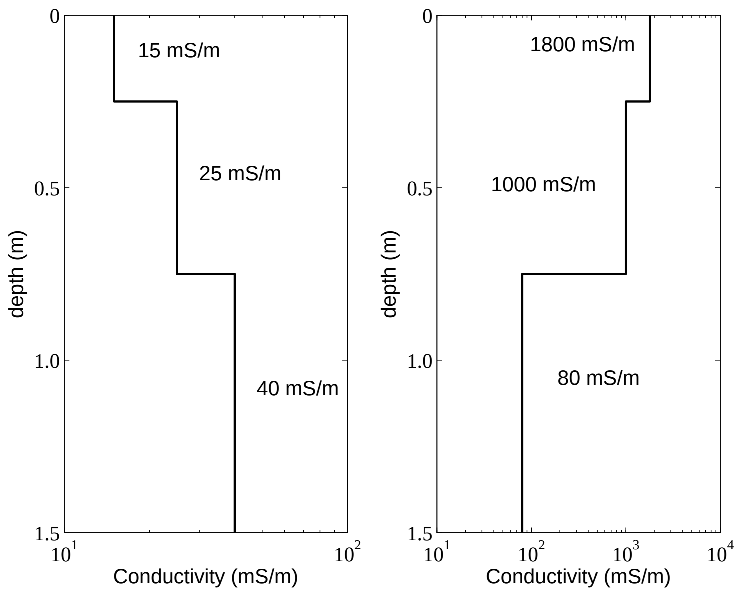

Fig. 1. Three-layer synthetic earth model of electrical conductivity for (a) non-saline soil and (b) saline soil in the top horizon.

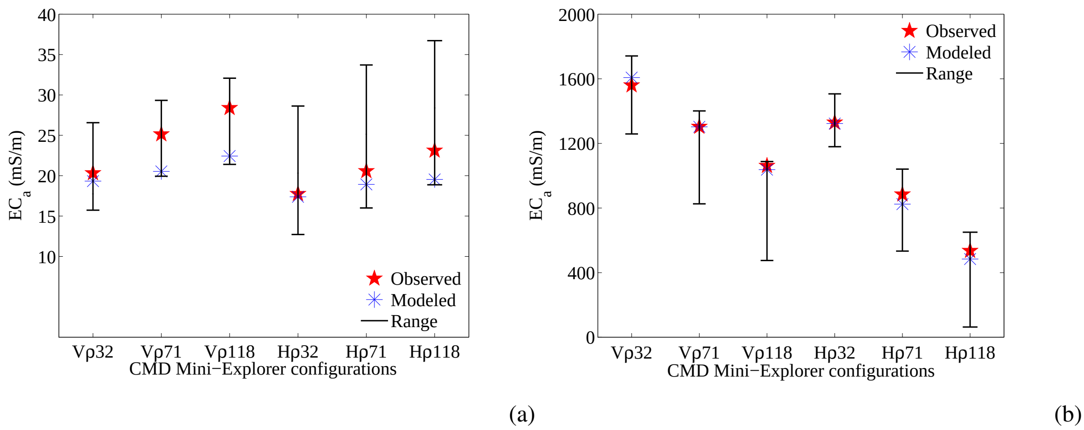

Fig. 2. Observed electrical conductivity obtained from the forward response of the six different configuration of CMD-Mini Explorer (red star), estimated (modeled) earth electrical conductivity (blue asterisk) and the range of EC_a simulated by MCMC for (a) non-saline and (b) saline soil scenarios.

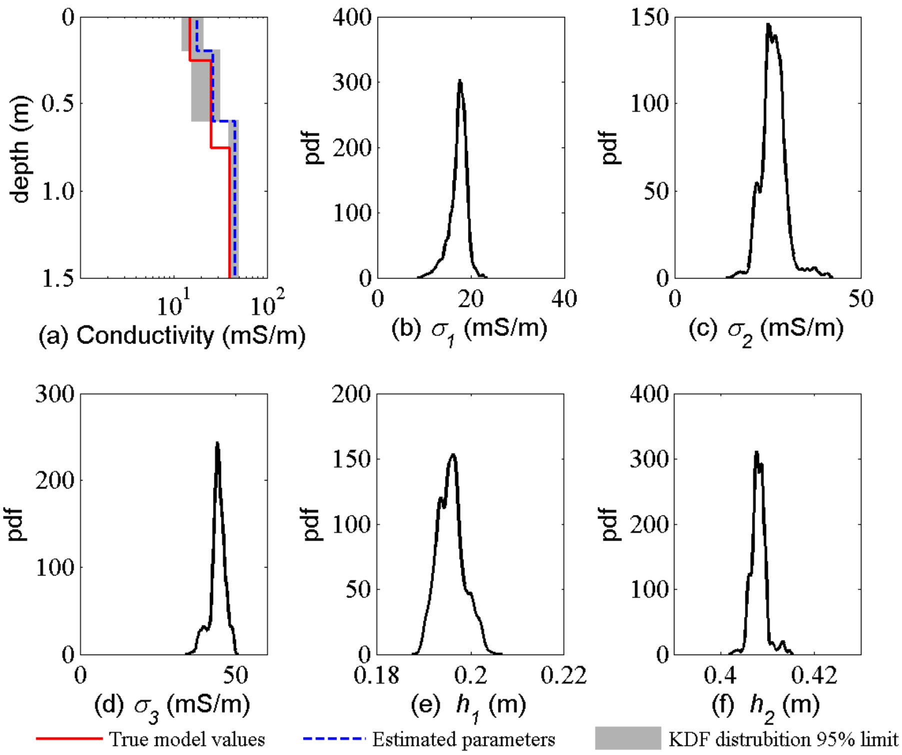

Fig. 3. Summary of the MCMC simulation for the synthetic three layer earth model of non-saline soil. (a) True (red line) and estimated parameter (blue dash-line) for the vertical electrical conductivity profile, and the gray background with the 95 percent confidence interval of kernel distribution estimation (KDE). (b − f) show the KDE of the marginalized posterior distributions for the three layer conductivities (σ_1, σ_2 and σ_3) and two layer thicknesses (h_1 and h_2).

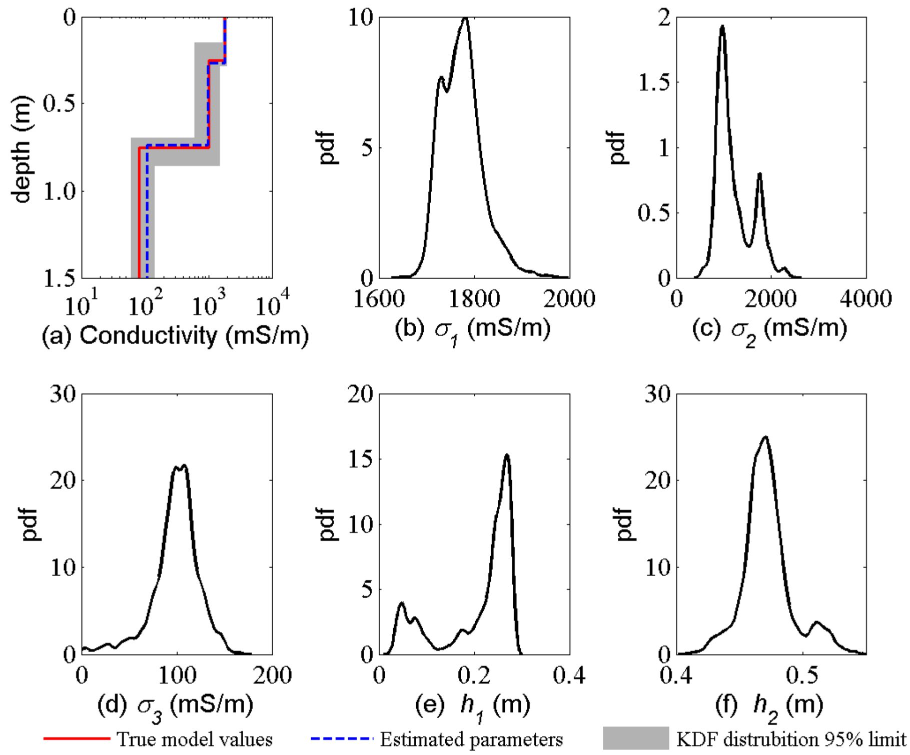

Fig. 4. Summary of the MCMC simulation for the synthetic three layer earth model of saline soil. (a) True (red line) and estimated parameter (blue dash-line) for the vertical electrical conductivity profile, and the gray background with the 95 percent confidence interval of kernel distribution estimation (KDE). (b − f) show the KDE of the marginalized posterior distributions for the three layer conductivities (σ_1, σ_2 and σ_3) and two layer thicknesses (h_1 and h_2).

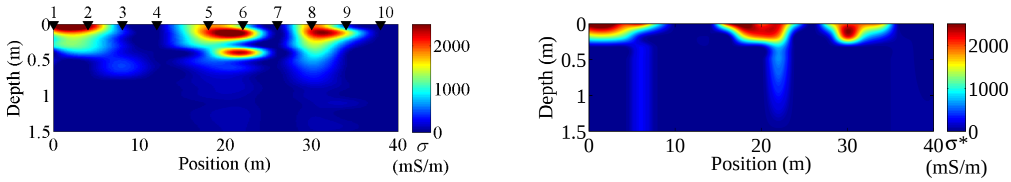

(a) (b)

Fig. 5. (a) electrical conductivity (mS/m) measured by the 5TE capacitance sensors from 10 soil pits along transect and the location of the soil pits is indicated by black triangles (Jadoon et al., 2015), (b) the soil electrical conductivity obtained by using Markov Chain Monte Carlo simulation for multi-configuration electromagnetic induction measurements.

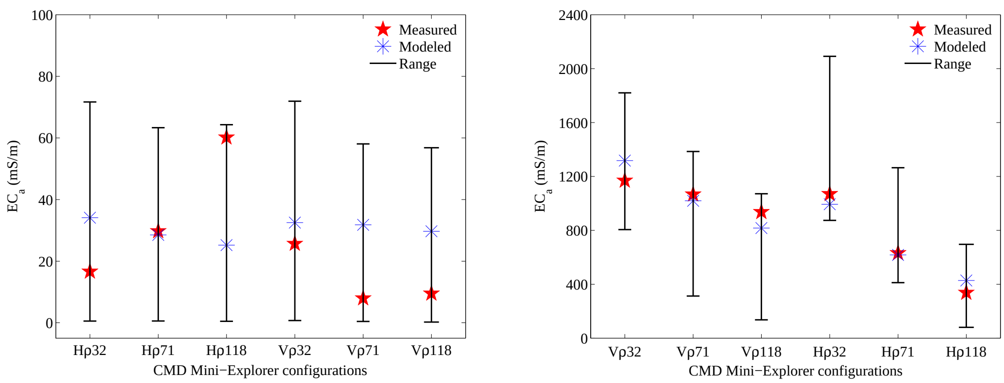

(a) (b)

Fig. 6. Measured six different configuration of CMD-Mini Explorer (red star), estimated (modeled) earth electrical conductivity (blue asterisk) and the range of EC_a simulated by MCMC for (a) non-saline soil at pit 4 and (b) saline soil at pit 9 location.

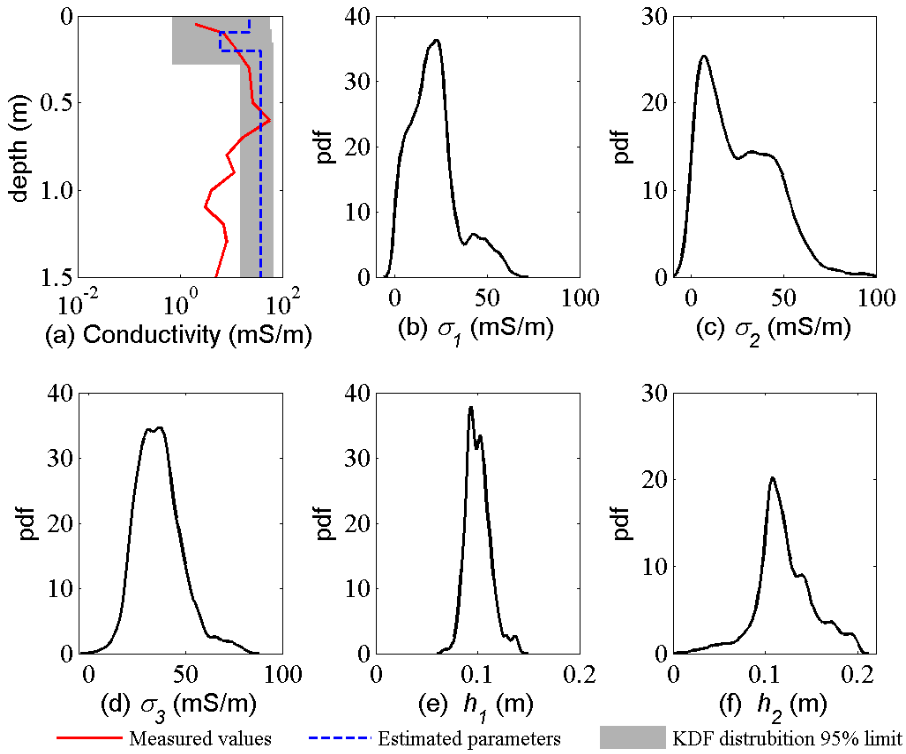

Fig. 7. Summary of the MCMC simulation for three-layer earth model by considering CMD-Mini explorer measurement over a non-saline soil. (a) True (red line) and estimated parameter (blue dash-line) for the vertical electrical conductivity profile, and the gray background with the 95 percent confidence interval of kernel distribution estimation (KDE). (b − f) show the KDE of the marginalized posterior distributions for the three layer conductivities (σ_1, σ_2 and σ_3) and two layer thicknesses (h_1 and h_2).

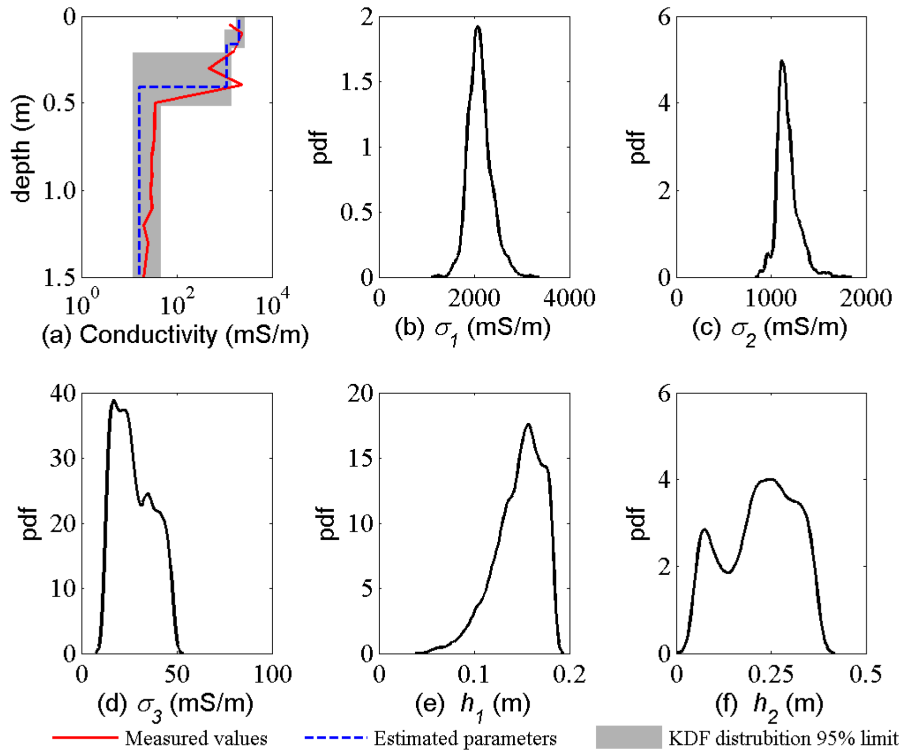

Fig. 8. Summary of the MCMC simulation for three-layer earth model by considering CMD-Mini explorer measurement over a saline soil. (a) True (red line) and estimated parameter (blue dash-line) for the vertical electrical conductivity profile, and the gray background with the 95 percent confidence interval of kernel distribution estimation (KDE). (b − f) show the KDE of the marginalized posterior distributions for the three layer conductivities (σ_1, σ_2 and σ_3) and two layer thicknesses (h_1 and h_2).

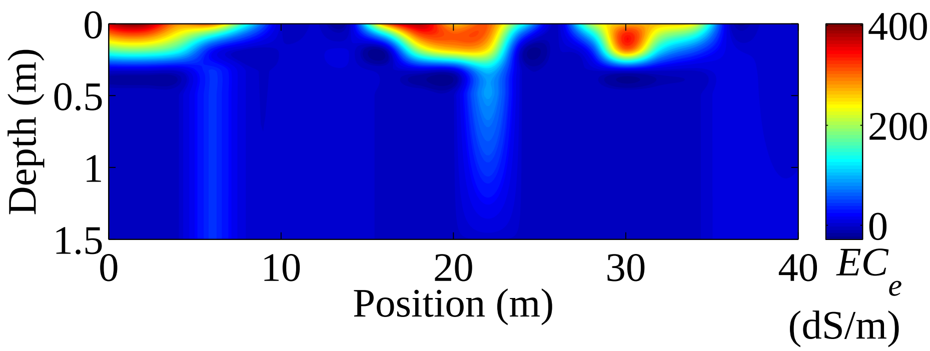

Fig. 9. Spatial distribution of soil salinity (EC_e) obtained using Bayesian inversion of multi-configuration EMI measurements along a transect.